

# ANALYSIS OF THE FAST-NEUTRON SPECTRUM INSIDE THE MATERIALS TEST BUNDLES IN THE NRU LOOPS

T.C. Leung

Atomic Energy of Canada Limited  
Reactor & Radiation Physics Branch  
Chalk River Laboratories  
Chalk River, Ontario  
K0J 1J0

## ABSTRACT

The 30-element Materials Test Bundles (MTB) in the NRU reactor provide a facility in which the effects of irradiation on CANDU\* reactor materials may be studied. Each bundle contains 1.71% enriched uranium in its 12-element inner fuel ring and 1.25% enriched uranium in its 18-element outer fuel ring. The MTB is installed in the high-flux position of a fuel string in the NRU loops, and supplies fast-neutron fluxes ( $E > 1$  MeV) up to  $5.3 \times 10^{17}$  n.m<sup>-2</sup>.s<sup>-1</sup>.

This paper describes how the MTB with its experimental insert was modeled to calculate the fast-neutron spectrum in the test bundle. Calculations were performed using the WIMS-AECL code, which is a multi-group transport code with two-dimensional capabilities using the collision probability method. Results of the fast-neutron spectrum above 1 MeV are presented in nine groups. The analysis confirms that the spectrum in the MTB is representative of the actual irradiation spectrum for fast-neutron damage in a CANDU reactor.

The calculated fast-neutron fluxes ( $E > 1$  MeV) at the specimen irradiation locations of the MTB were compared with integral measurements that were obtained from iron-wire flux monitors by determining the Mn<sup>54</sup> activities arising from the Fe<sup>54</sup>(n,p) Mn<sup>54</sup> reaction. The measured and calculated values for the fast-neutron fluxes agree to within 12%.

## 1. INTRODUCTION

In the material research program on CANDU reactor fuel channels, it is essential to determine material properties that cover up to the 30-year lifetime of the reactor core components [1]. The materials of specific interest are zirconium and its alloys, which are used in the pressure tubes and calandria tubes of CANDU reactors. At Chalk River Laboratories (CRL), particular research emphasis has been placed on fast-neutron radiation damage studies and our ability to predict in-reactor deformation and metallurgical behaviour changes for reactor materials subject to high neutron fluence over  $10^{25}$  n.m<sup>-2</sup>. Current in-reactor test programs include experiments on irradiation creep and growth, corrosion, and compact toughness and tensile strength of material specimens [2-4].

---

\* CANDU: CANada Deuterium Uranium; registered trademark.

The NRU reactor at CRL provides three irradiation facilities to study the effects of fast neutrons on reactor materials at various flux levels. The facilities comprise two types of fast neutron (FN) rods and one type of Materials Test Bundles (MTB). The two types of FN rods used in NRU are the Mk4 and Mk7 FN rods. The former uses natural uranium and provides fast-neutron fluxes ( $E > 1$  MeV) up to  $2.1 \times 10^{17}$  n.m<sup>-2</sup>.s<sup>-1</sup>. The latter uses enriched uranium and is in the prototype stage, providing fast-neutron fluxes up to  $6.8 \times 10^{17}$  n.m<sup>-2</sup>.s<sup>-1</sup>. The MTB uses slightly enriched uranium (1.25 and 1.71 wt% U-235), and provides fast-neutron fluxes of approximately  $5.3 \times 10^{17}$  n.m<sup>-2</sup>.s<sup>-1</sup>.

With increasing requirements for quantitative evaluation of fast fluxes to cross-correlate results from different test reactors, and to assess their applicability to CANDU power reactors, more accurate assessments of fast fluxes in our irradiation facilities are required [5]. It is therefore necessary to determine the total fast-neutron flux above 1 MeV and the fast-neutron spectrum at the specimen irradiation locations inside the FN rods and the MTB in NRU. The fast-neutron spectral analyses for the Mk4 and Mk7 FN rods have been completed and documented [6,7]. This paper describes a similar type of analysis for the fast-neutron spectrum inside the MTB, and presents some results from integral fast-neutron flux measurements ( $E > 1$  MeV) for comparison.

## 2. THE MATERIALS TEST BUNDLES IN THE NRU LOOPS

The NRU reactor is heavy water cooled and moderated, with an on-line refueling capability. It is licensed to operate at a maximum power of 135 MW, with a peak thermal flux of approximately  $4.0 \times 10^{18}$  n.m<sup>-2</sup>.s<sup>-1</sup> [8].

The NRU loops are high-temperature and high-pressure test facilities, in which test elements may be subjected to conditions simulating those existing in power reactors. The loops are used mainly for power reactor fuel development, for material testing, and for studying fuel behavior under accident conditions. Figure 1 shows schematically a typical NRU loop, with a fuel string of six test fuel bundles in it. The loop test section is confined to a 10.3 cm ID pressure tube, which is made of Zr-2.5%Nb or other Zircaloy alloys. The design pressure and temperature of the U1 and U2 loops are 13.9 MPa and 354<sup>o</sup>C, respectively. The loops are cooled by light water, and the flow rates for the U1 and U2 loops are 17 and 20 kg/s, respectively. The nominal axial peak thermal flux at the cell boundary of the U1 or U2 loop is  $3 \times 10^{18}$  n.m<sup>-2</sup>.s<sup>-1</sup> [8].

The MTB was designed to enable metallurgical specimens to be irradiated at a high-flux position in an NRU loop, such as the two middle positions on a loop fuel string, as shown in Figure 1. The MTB can be installed on an NRU loop fuel string without modifications to any existing fuel-string hardware. It is a 30-element bundle, which has a modified 600 MW CANDU fuel-bundle design [9]. Figure 2 shows a cross-section of an MTB, which has an overall length of 482 mm. Its outer fuel ring has 18 elements with uranium enriched to 1.25 wt% U-235, and its inner ring has 12 elements with uranium enriched to 1.71 wt% U-235. The center seven elements of the bundle have been removed and replaced by a 41.7 mm ID, 43.2 mm OD Zircaloy tube welded to the webs of the end plates. This tube provides internal support to the bundle and serves as a guide for the specimen-holder assembly.

There are at present two types of specimen-holder assemblies for the MTB. The first type is designed for irradiation growth and creep specimens. It consists of six individual specimen-holder tubes, which resemble the six elements removed from the second center fuel ring of a standard 600 MW CANDU bundle. Another type of specimen-holder assembly is designed for irradiating compact toughness, tensile, and cantilever beam specimens. It has four components: a sleeve, a triangular tube, a circular end-plate and a triangular end-plate. The specimens are hung from the pins projecting from the outer surface of the triangular tube, and the sleeve is slid over the triangular tube. Each type of specimen-holder assembly can be inserted into the Zircaloy support tube of the MTB with adequate space in-between for cooling water flow.

### 3. METHOD OF ANALYSIS

The present study for the MTB used a super-cell model, which included the cell-of-interest and its neighbouring fuel rods, as shown in Figure 3. The neighbouring fuel rods provided the correct driving spectrum for the MTB, and were modeled as two fuel rings located at radii of 19.2 and 38.9 cm from the center of the cell. The fuel loadings in the first and second driver-fuel rings were about 2 g/cm and 4 g/cm of U-235, respectively. A boron-10 ring was added outside the fuel ring, to keep the super-cell k-effective close to 1.0.

The experimental insert was modeled as three annuli: the first for the center hanger bar, the second for the specimen-holder assembly and specimens, and the third for the Zircaloy support tube. The three annuli were separated by the water coolant in the pressure tube. The radii and material composition of the second annulus may vary slightly, depending on which type of specimen-holder assembly is used. Details of the MTB as modeled for the computer calculations are shown in Figures 2 and 3.

The neutron-flux calculations for the MTB were performed using the WIMS-AECL [10] code, with its associated ENDF/B-V derived data base [11]. WIMS-AECL is a multigroup transport code with two-dimensional capabilities using the 'Pij' collision probability method. The main transport calculations were performed using 34 energy group subdivisions, with nine groups above 1 MeV. The computation work was performed using the SGI Challenge-L computer at CRL.

### 4. CALCULATED FAST-NEUTRON SPECTRUM

Table 1 lists the calculated neutron-flux spectrum at the specimen irradiation locations of the MTB. The MTB neutron fluxes are normalized to a nominal thermal flux of  $2.85 \times 10^{18} \text{ n.m}^{-2}.\text{s}^{-1}$  in the first driver-fuel ring. This is equivalent to normalizing to a linear bundle fission power of 1.73 MW/m, or a total bundle fission power of approximately 834 kW. The linear fission powers of the fuel elements in the inner and outer rings are 58.5 and 57.1 kW/m, respectively. In Table 1, the fast-neutron flux above 1 MeV in the MTB is calculated to be  $5.31 \times 10^{17} \text{ n.m}^{-2}.\text{s}^{-1}$ . Using the same method of analysis, the fast-neutron fluxes provided by the NRU Mk4 and Mk7 FN rods were calculated to be 2.07 and  $6.82 \times 10^{17} \text{ n.m}^{-2}.\text{s}^{-1}$ , respectively [6,7]. Thus, the MTB provides a materials irradiation facility at a fast-neutron flux level between those of the Mk4 and Mk7 FN rods.

In Table 1, the percentages of neutron fluxes in each group of the MTB spectrum are compared with those of the Mk7 and Mk4 FN rods [6,7], and those in the pressure tube and calandria tube of a fuel channel containing 37-element CANDU fuel bundles [12]. For each spectrum, the sum of the neutron fluxes of all energy groups was normalized to be 100%. For the MTB, the percentage of neutron flux above 1 MeV is 15.6%, and for the Mk7 FN rod, the Mk4 FN rod, the pressure tube, and calandria tube, it is 13.1, 6.5, 7.4 and 5.6%, respectively.

Of the five spectra in Table 1, the MTB has the highest percentage of fast neutrons ( $E > 1 \text{ MeV}$ ). However, if only the energy spectrum above 1 MeV is considered, the flux distributions for all five cases are very similar. For further comparison, the fluxes in the first nine energy groups of each distribution are shown in Figure 4. In each case, the sum of the neutron group fluxes between 1 and 10 MeV is normalized to 100%. The spectral shapes for all five cases are in good agreement. The Mk7 FN rod has the largest group flux deviation from the MTB, which is about 6.3% for neutron energies between 1.05 and 1.35 MeV.

## 5. FAST-NEUTRON FLUX MEASUREMENT

### 5.1 Iron-Wire Flux Monitors

Iron-wire flux monitors are used for the fast-neutron flux measurements ( $E > 1$  MeV) in the MTB. The reaction  $\text{Fe}^{54}(n,p)\text{Mn}^{54}$  has an effective threshold at approximately 1.05 MeV. The measured activity of  $\text{Mn}^{54}$ , which has a 312.5-day half-life, can be used to determine the fast-neutron flux above 1 MeV. The measured activity of  $\text{Mn}^{54}$  is first corrected for counter efficiency to obtain the absolute activity. The absolute activity per unit mass,  $A$ , is related to the fast-neutron flux ( $E > 1$  MeV) by:

$$A = N\sigma_{FE}\phi(1 - \exp(-\lambda t_1)) \exp(-\lambda t_2) \quad (1)$$

where  $N$  is the number of iron atoms per unit mass of wire,

$t_1$  is the irradiation time in the reactor at an assumed constant flux,  $\phi$ ,

$t_2$  is the counting delay time after irradiation, and

$\lambda$  is the decay constant of  $\text{Mn}^{54}$ .

$\sigma_{FE}$  is the effective or spectrum-averaged iron cross-section, which can be written as

$$\sigma_{FE} = \sum \sigma_i \phi_i / \sum \phi_i, \text{ summed over the energy groups above 1 MeV.} \quad (2)$$

$\sigma_i$  and  $\phi_i$  are the group cross-sections for iron and group fluxes of the neutron spectrum at the irradiation location of the material specimens. In this case, the WIMS-calculated fast-neutron spectrum at the specimen irradiation locations inside the MTB is used to calculate the effective or spectrum-averaged cross-section of the iron-wire flux monitor.

The  $\text{Fe}^{54}(n,p)\text{Mn}^{54}$  reaction has a significant cross-section at energies greater than 10 MeV, but the present WIMS group structure is limited to 10 MeV. In order to generate the group fluxes for energies above 10 MeV, the WIMS-calculated nine-group fluxes from 1.05 to 10 MeV are first curved-fitted and then extrapolated to cover the energy range from 10 to 20 MeV. The fitted fluxes can be described by a fission spectrum of the form:

$$\phi(E) = \phi_0 E^{1/2} \exp(-E/T) \quad (3)$$

where  $\phi_0$  and  $T$  are fitted parameters.

Table 2 shows how the effective iron cross-section is calculated for energies between 1.05 and 20 MeV. The group cross-section data of iron were taken from Reference 13. Since the contribution for energy groups above 10 MeV is only 0.5% of the total effective cross-section, any error introduced in the flux extrapolation procedure will not significantly affect the final result of the iron cross-section. From Table 2, the effective iron cross-section inside the MTB is calculated to be  $101.5 \pm 3$  mb.

### 5.2 Comparison of Measured and Calculated Fast-Neutron Fluxes

Integral measurements of the fast-neutron fluxes above 1 MeV have been obtained from a Materials Test Bundle, AHA, which was irradiated in axial position 3 of the U1B-242 fuel-string assembly in the U1 loop of NRU at site L08, from 1994 February 12 to 1994 July 9. The irradiation was part of an on-going program to study the irradiation creep and growth of Zirconium pressure tube alloys. The experimental insert of the bundle contained iron-wire flux monitors in three of the specimen holders, attached to their upper, middle and lower sections. In irradiation position 3 (see Figure 1), the lower section was closest to the center of the

reactor, and therefore had the highest flux. The iron-wire flux monitor was 0.25 mm in diameter by 2.54 cm long. Data for the iron-wire flux measurements were obtained from R. J. Klassen and F. J. Butcher at CRL.

The fast-neutron fluxes above 1 MeV were measured by determining the  $\text{Mn}^{54}$  activities, arising from the  $\text{Fe}^{54}(n,p)\text{Mn}^{54}$  reaction from iron-wire flux monitors, irradiated over the same period of time in 1994. Using Eq. (1), and an effective iron cross-section of 101.5 mb from the last section, the measured fast-neutron fluxes averaged over the irradiation period in the upper, middle and lower sections of the specimen holders were determined to be  $4.34$ ,  $4.53$  and  $4.68 \times 10^{17} \text{ n.m}^{-2}.\text{s}^{-1}$ , respectively.

The fast-neutron fluxes at the same specimen-holder locations of the AHA bundle were also calculated using the WIMS-AECL code. The calculated fluxes were normalized using the average linear heat ratings of 53.73, 55.84 and 56.87 kW/m for the upper, middle and lower sections of the inner fuel ring elements of the MTB, respectively. The linear heat ratings were obtained from the BURFEL code calculations [14], using total loop power measurements taken from the same period of irradiation as the iron-wire flux monitors, and using an appropriate fitted axial-flux profile to evaluate the MTB powers in the fuel string. A power-to-coolant ratio of 0.97 was used to convert the linear heat ratings to linear fission power ratings for the three sections of the MTB fuel elements. In the calculation, a burnup effect correction was also made, and the percent of fast neutrons ( $E > 1 \text{ MeV}$ ) in the whole spectrum dropped from 15.6% for a fresh fuel to 15.2% for a fuel with about 100 MWd burnup. The calculated fast-neutron fluxes ( $E > 1 \text{ MeV}$ ) in the upper, middle and lower sections of the specimen holders were calculated to be  $4.89$ ,  $5.08$  and  $5.17 \times 10^{17} \text{ n.m}^{-2}.\text{s}^{-1}$ , respectively.

Table 3 compares the measured and calculated fast-neutron fluxes of the AHA bundle at the three elevations. In general, the calculated and measured values agree to within 12%. The accuracy of the measured fast-neutron fluxes was estimated to be about  $\pm 8\%$ , with  $\pm 5\%$  for the  $\text{Mn}^{54}$  activity measurements and  $\pm 3\%$  for the effective iron cross-section. The accuracy of the calculated fluxes was estimated to be about  $\pm 15\%$ , due to large uncertainties in evaluating the average linear heat ratings of the fuel elements of the MTB bundle, irradiated with several other fuel bundles in a fuel string. The accuracy of the calculated fluxes for other MTB bundles might be better if the accuracy of the bundle linear heat ratings determined by BURFEL can be improved.

## 6. CONCLUSIONS

The main conclusions of this study are:

1. The MTB provides an fast-neutron irradiation facility at a flux level between those of the Mk4 and Mk7 FN rods in NRU. At a bundle fission power of 834 kW, or linear fission power rating of 1.73 MW/m, the fast-neutron flux ( $E > 1 \text{ MeV}$ ) at the irradiation locations of the MTB was calculated to be  $5.3 \times 10^{17} \text{ n.m}^{-2}.\text{s}^{-1}$ .
2. The fast-neutron flux distribution above 1 MeV in an MTB is in good agreement with those of a Mk4 rod, a Mk7 rod and a CANDU fuel-bundle pressure tube and calandria tube, to within 6.3%.
3. The effective or spectrum-averaged iron cross-section for the MTB was determined to be  $101.5 \pm 3 \text{ mb}$ .
4. The measured and calculated fast-neutron fluxes ( $E > 1 \text{ MeV}$ ) at the specimen irradiation locations of the MTB agree to within 12%.

## 7. ACKNOWLEDGMENTS

The work described in this report was funded by the CANDU Owners Group, WPIR No. 3210, Working Party 32.

The author would like to thank N. Christodoulou and M. Miller for initiating this study, and M.D. Atfield for supervising the analysis.

## 8. REFERENCES

- [1] J.T. Dunn, "CANDU 600 Fuel Channels Assessment of Pressure Tube Failure at Pickering 'A' ", AECL report, TDAI-362, 1984 June.
- [2] V. Fidleris, "The Irradiation Creep and Growth Phenomena", Journal of Nuclear Materials, 159, pp22-42, 1988.
- [3] A.R. Causey, F.J. Butcher and S.A. Donohue, "Measurement of Irradiation Creep of Zirconium Alloys using Stress Relaxation", Journal of Nuclear Materials, 159, pp 101-103, 1988.
- [4] M.A. Miller, Unpublished report, 1995 August.
- [5] T.S. Gendron, R.A. Holt and R.G. Fleck, "Materials Irradiations in CANDU Fuel Bundles", AECL report, AECL-10632, 1992 May.
- [6] T.C. Leung, "Analysis of The Fast-Neutron Spectrum Inside the Experimental Cavity of the NRU Mk4 FN Rod", Proceedings of the 19<sup>th</sup> CNS Simulation Symposium, Hamilton, 1995 October.
- [7] T.C. Leung, Unpublished report, 1997 January.
- [8] D.T. Nishimura, "Summary of Loops in Chalk River NRX and NRU Reactors", AECL report, AECL-6980, 1980 December.
- [9] L.N. Herbert and T.J. Carter, Unpublished report, 1980 August.
- [10] J.V. Donnelly, "WIMS-AECL, A User's Manual for the Chalk River Version of WIMS", AECL report, AECL-8955, 1986 January.
- [11] G.L. Festarini, Unpublished report, 1985 April.
- [12] R.E. Donders, Unpublished report, 1988 March.
- [13] M.B. Zeller, Unpublished report, 1991 January.
- [14] J.E. Baird and W. Heeds, Unpublished report, 1996 December.

Table 1: Comparison of Neutron Spectra Between the NRU MTB, Mk7 and Mk4 FN Rods, and the Pressure and Calandria Tubes of a CANDU Fuel Channel.

G R O U P	ENERGY WIDTH	NRU MTB FLUX	NRU MTB FLUX	NRU Mk7 FN ROD FLUX	NRU Mk4 FN ROD FLUX	PT FLUX of CANDU FUEL CHANNEL	CT FLUX of CANDU FUEL CHANNEL
	MeV	$\times 10^{16}$ $n.m^{-2}.s^{-1}$	%	%	%	%	%
1	7.79-10.0	0.420	0.124	0.110	0.055	0.060	0.045
2	6.07-7.79	1.184	0.348	0.306	0.157	0.175	0.132
3	4.72-6.07	2.675	0.787	0.690	0.350	0.392	0.298
4	3.68-4.72	4.483	1.318	1.156	0.573	0.647	0.488
5	2.87-3.68	6.777	1.993	1.723	0.858	0.973	0.741
6	2.23-2.87	8.956	2.634	2.250	1.129	1.306	0.995
7	1.74-2.23	9.024	2.653	2.268	1.095	1.236	0.935
8	1.35-1.74	9.846	2.896	2.364	1.162	1.302	0.998
9	1.05-1.35	9.744	2.865	2.256	1.121	1.265	0.979
	<b>Sub-total</b>	<b>[53.109]</b>	<b>[15.618]</b>	<b>[13.123]</b>	<b>[6.500]</b>	<b>[7.356]</b>	<b>[5.611]</b>
10	0.82-1.05	9.625	2.830	2.131	1.087	1.246	0.991
11	0.64-0.82	10.422	3.065	2.212	1.183	1.509	1.207
12	0.50-0.64	8.645	2.542	1.892	1.003	1.321	1.065
13	0.39-0.50	6.265	1.842	1.475	0.748	0.914	0.767
14	0.30-0.39	7.131	2.095	1.655	0.876	1.232	1.062
15	0.24-0.30	6.184	1.819	1.523	0.801	1.213	1.062
16	0.18-0.24	5.408	1.590	1.363	0.723	1.151	1.021
17	0.14-0.18	4.717	1.387	1.185	0.648	1.088	0.976
18	0.11-0.14	4.259	1.253	1.194	0.620	1.043	0.954
	<b>Sub-total</b>	<b>[62.656]</b>	<b>[18.423]</b>	<b>[14.630]</b>	<b>[7.689]</b>	<b>[10.717]</b>	<b>[9.105]</b>
19	$0.625 \times 10^{-6}$ -0.11	101.782	29.931	32.438	19.811	25.171	25.425
Th.	Below $0.625 \times 10^{-6}$	122.519	36.028	39.809	66.000	56.756	59.859
	<b>Total</b>	<b>340.066</b>	<b>100.000</b>	<b>100.000</b>	<b>100.000</b>	<b>100.000</b>	<b>100.000</b>

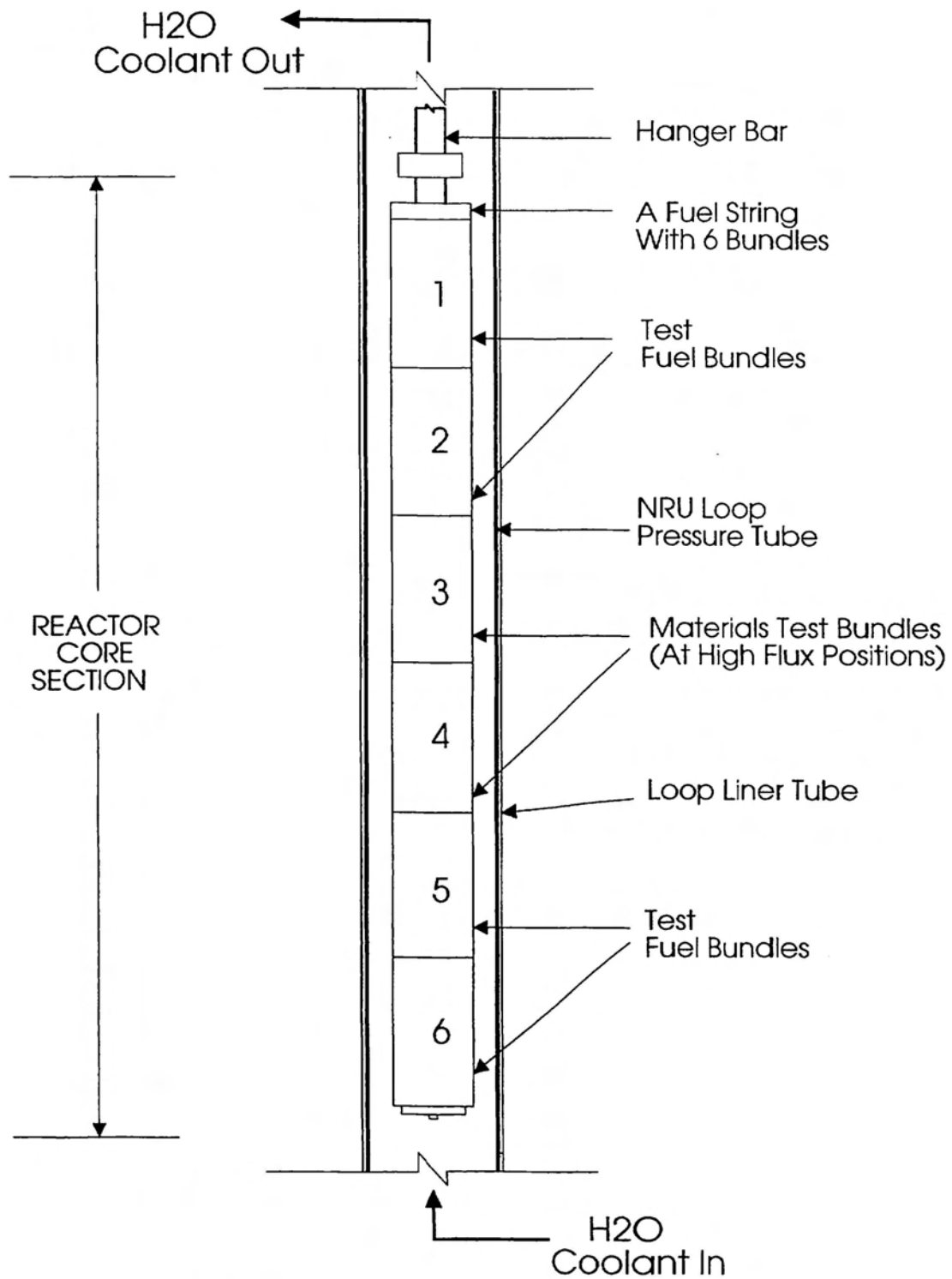
Table 2: Calculation of the Effective Iron Cross-section At the Specimen Irradiation Locations of the NRU MTB

LOWER ENERGY MeV	UPPER ENERGY MeV	IRON CROSS-SECTION mb	FLUX-WEIGHTING FACTOR	WEIGHTED IRON CROSS-SECTION mb
1.05	1.35	$7.54 \times 10^{-1}$	$1.83 \times 10^{-1}$	$1.38 \times 10^{-1}$
1.35	1.74	$3.27 \times 10^0$	$1.85 \times 10^{-1}$	$6.05 \times 10^{-1}$
1.74	2.23	$2.12 \times 10^1$	$1.70 \times 10^{-1}$	$3.60 \times 10^0$
2.23	2.87	$7.56 \times 10^1$	$1.68 \times 10^{-1}$	$1.27 \times 10^1$
2.87	3.68	$1.90 \times 10^2$	$1.27 \times 10^{-1}$	$2.41 \times 10^1$
3.68	4.72	$2.93 \times 10^2$	$8.43 \times 10^{-2}$	$2.47 \times 10^1$
4.72	6.07	$4.13 \times 10^2$	$5.03 \times 10^{-2}$	$2.08 \times 10^1$
6.07	7.79	$4.69 \times 10^2$	$2.22 \times 10^{-2}$	$1.04 \times 10^1$
7.79	10.00	$4.77 \times 10^2$	$7.93 \times 10^{-3}$	$3.78 \times 10^0$
10.00	11.91	$4.69 \times 10^2$	$1.26 \times 10^{-3}$	$5.91 \times 10^{-1}$
11.91	13.50	$4.20 \times 10^2$	$2.79 \times 10^{-4}$	$1.17 \times 10^{-1}$
13.50	14.92	$3.47 \times 10^2$	$7.91 \times 10^{-5}$	$2.74 \times 10^{-2}$
14.92	16.91	$2.49 \times 10^2$	$3.00 \times 10^{-5}$	$7.47 \times 10^{-3}$
16.91	20.00	$1.55 \times 10^2$	$6.57 \times 10^{-6}$	$1.02 \times 10^{-3}$
	<b>Total</b>		<b>1.000</b>	<b>101.5 mb *</b>

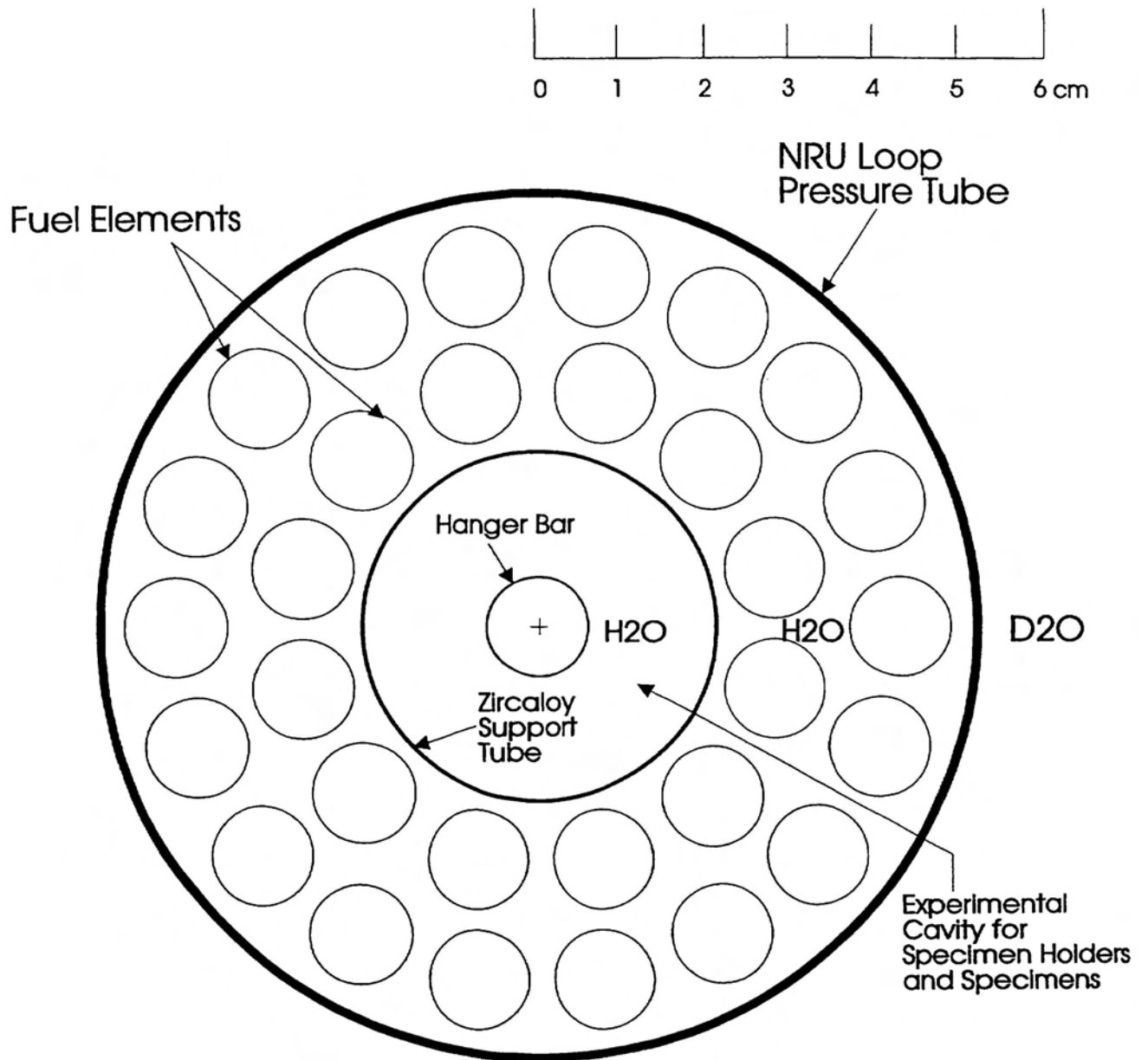
\* The uncertainty for the effective iron cross-section is estimated to be  $\pm 3$  mb.

Table 3: Comparison of Measured and Calculated Fast-Neutron Fluxes ( $E > 1$  MeV) at Specimen-Holder Locations of the AHA Materials Test Bundle in NRU.

ELEVATION	MEASURED FAST NEUTRON FLUXES IN 3 SPECIMEN HOLDERS			AVERAGED MEASURED FAST NEUTRON FLUXES ( $\sim \pm 8\%$ ) $\times 10^{17} \text{ n.m}^{-2} \cdot \text{s}^{-1}$	CALCULATED FAST NEUTRON FLUXES ( $\sim \pm 15\%$ ) $\times 10^{17} \text{ n.m}^{-2} \cdot \text{s}^{-1}$	DEVIATION OF MEASURED FLUXES FROM CALCULATION
	A	B	C			
UPPER	4.27	4.38	4.38	4.34	4.89	-11.2%
MIDDLE	4.49	4.61	4.49	4.53	5.08	-10.8%
LOWER	4.61	4.83	4.61	4.68	5.17	-9.5%



**Figure 1: A Typical NRU Loop with a Fuel String of 6 Fuel Bundles**



**Figure 2: Cross-section of an Materials Test Bundle**

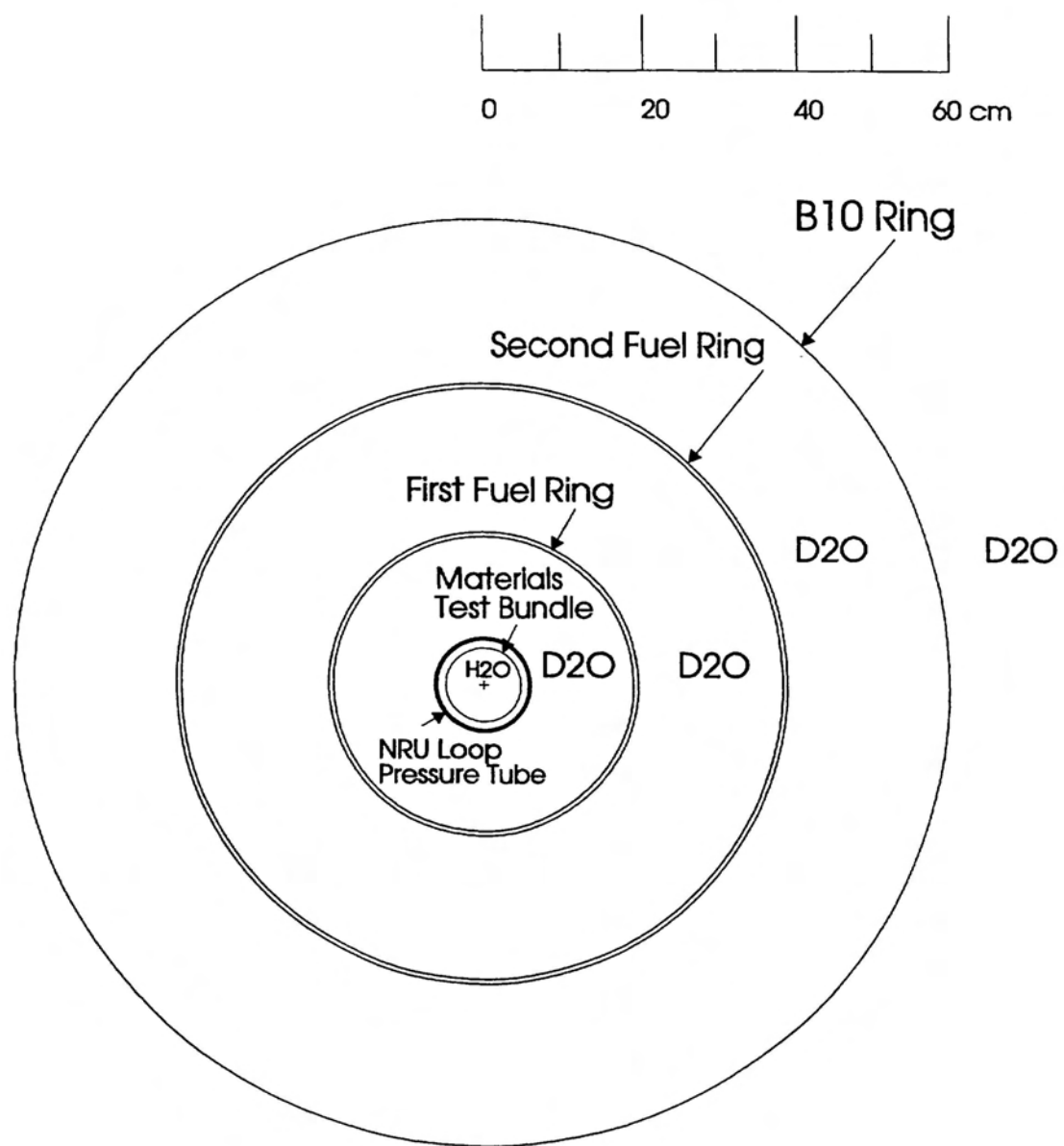


**Figure 3: Sketch of the Super-cell Model for the MTB Analysis**

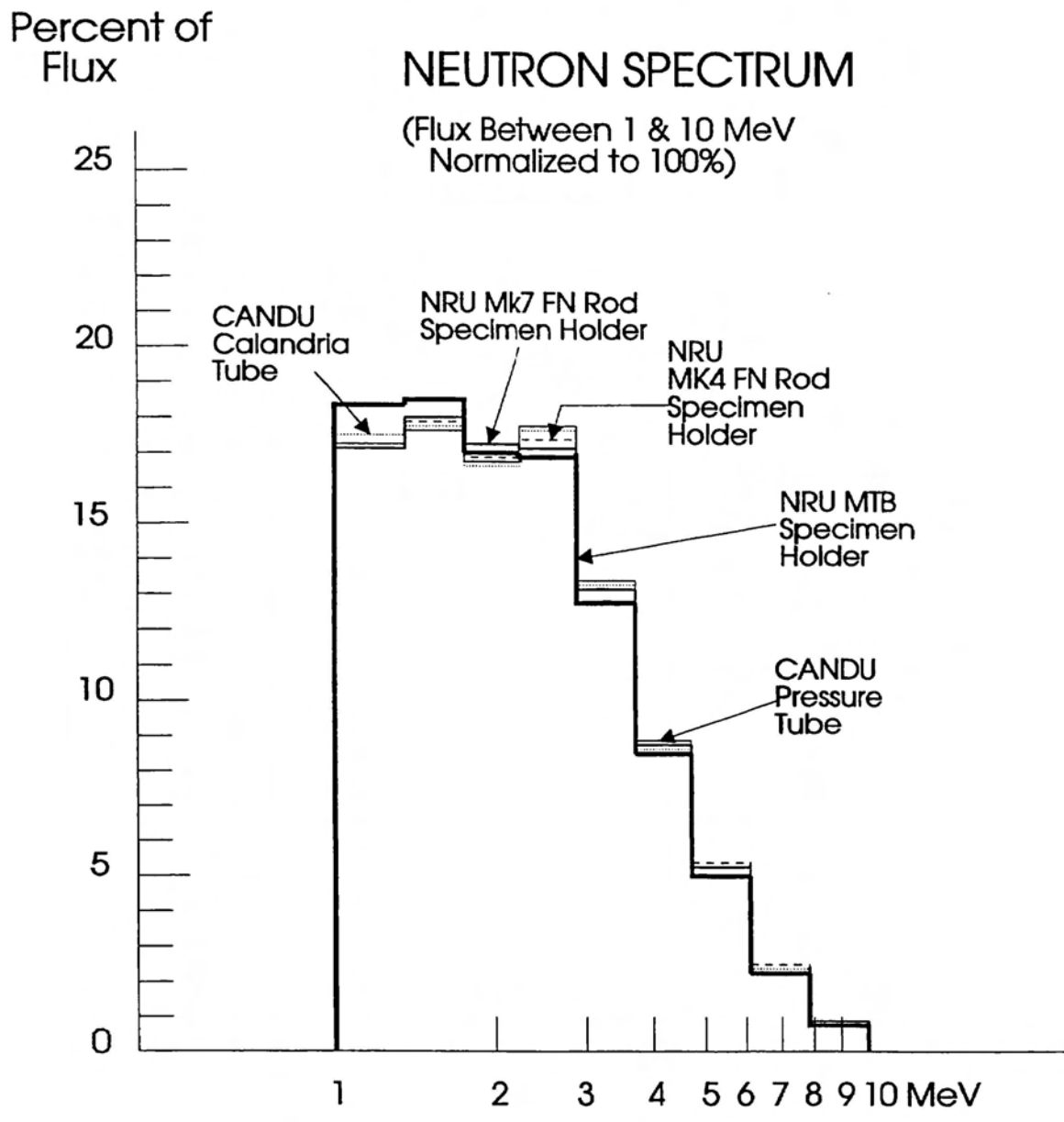


Figure 4: Comparison of Fast-Neutron Distributions Above 1 MeV